Cell

Sec22b Regulates Phagosomal Maturation and Antigen Crosspresentation by Dendritic Cells

Ignacio Cebrian,[1] Geraldine Visentin,[1] Nicolas Blanchard,[2] Mabel Jouve,[5] Alexandre Bobard,[3] Catarina Moita,[4] Jost Enninga,[3] Luis F. Moita,[4] Sebastian Amigorena,[1,*] and Ariel Savina[1,*]

[1]Institut Curie, INSERM U932, Immunité et Cancer, 26 rue d'Ulm, 75248 Paris Cedex 05, France

[2]Centre de Physiopathologie de Toulouse-Purpan INSERM UMR1043-CNRS UMR5282, Université de Toulouse III CHU Purpan BP 3028, 31024 Toulouse Cedex 3, France

[3]Institut Pasteur, Dynamique des Interactions Hôte-Pathogène, Paris 75724, France

[4]Cell Biology of the Immune System Unit, Instituto de Medicina Molecular, Faculdade de Medicina, Universidade de Lisboa, 1649-028 Lisboa, Portugal

[5]Institut Jacques Monod, UMR7592 CNRS/Université Paris Diderot, ImagoSeine-Plateforme de Microscopie Electronique, 75205 Paris Cedex 13, France

*Correspondence: sebastian.amigorena@curie.fr (S.A.), ariel.savina@curie.fr (A.S.)

DOI 10.1016/j.cell.2011.11.021

SUMMARY

Antigen (Ag) crosspresentation by dendritic cells (DCs) involves the presentation of internalized Ags on MHC class I molecules to initiate CD8+ T cell-mediated immunity in response to certain pathogens and tumor cells. Here, we identify the SNARE Sec22b as a specific regulator of Ag crosspresentation. Sec22b localizes to the ER-Golgi intermediate compartment (ERGIC) and pairs to the plasma membrane SNARE syntaxin 4, which is present in phagosomes (Phgs). Depletion of Sec22b inhibits the recruitment of ER-resident proteins to Phgs and to the vacuole containing the *Toxoplasma gondii* parasite. In Sec22b-deficient DCs, crosspresentation is compromised after Ag phagocytosis or endocytosis and after invasion by *T. gondii*. Sec22b silencing inhibited Ag export to the cytosol and increased phagosomal degradation by accelerating lysosomal recruitment. Our findings provide insight into an intracellular traffic pathway required for crosspresentation and show that Sec22b-dependent recruitment of ER proteins to Phgs critically influences phagosomal functions in DCs.

INTRODUCTION

Dendritic cells (DCs) are the most potent antigen (Ag)-presenting cells that can initiate adaptive immune responses. To do so, DCs process and present Ags in the context of class I or class II MHC molecules to trigger CD8+ or CD4+ T cell responses, respectively. Contrary to MHC class II presentation that is almost restricted to exogenous Ags, the MHC class I presentation involves both endogenous—classic pathway—and exogenous internalized Ags. The latter, referred as "crosspresentation," is important to establish CD8+ cytotoxic immune responses against tumor cells, bacteria, or virus that not infect DCs. DCs have developed a strong specialization of their internalization pathway that allows them to crosspresent Ags more efficiently than other phagocytes. Indeed, contrary to macrophages, which acidify their phagosomes (Phgs) very rapidly, the phagocytic pathway of DCs acidifies very slowly and inefficiently due to both the phagosomal production of reactive oxygen species by the NADPH oxydase NOX2 (Savina et al., 2006) and to an incomplete activation of the V-ATPase (Trombetta et al., 2003). High pH, together with lower levels of lysosomal proteases (Delamarre et al., 2005), limits the levels of proteolysis in DC Phgs (Savina et al., 2006; Jancic et al., 2007; Savina and Amigorena, 2007). Limited proteolysis most likely preserves intact proteins or large polypeptides for export into the cytosol, where these Ags are degraded by the proteasome. The processed peptides are then translocated by TAP1/2 peptide transporters into the lumen of the ER or back into phagosomes (that have recruited ER components) (Kovacsovics-Bankowski and Rock, 1995). After translocation, peptides are trimmed by ER-resident aminopeptidases and their analogs, such as IRAP (Saveanu et al., 2009), and are loaded on class I MHC molecules by the ER "peptide loading complex," which includes tapasin, calreticulin (Crt), calnexin, and ERp57 (Wearsch and Cresswell, 2007). MHC class I-peptide complexes are then transported to the cell surface to finally stimulate CD8+ T cells.

Although we do have a global view of crosspresentation in terms of the intracellular pathways (review in Amigorena and Savina, 2010), the molecular mechanisms that regulate the intracellular membrane trafficking during this process are still incompletely understood. In fact, internalized Ags have to supply both crosspresentation and MHC class II presentation; however, how these two pathways with different Ag processing requirements are spatial and temporally coordinated by DCs is unclear. For instance, one of the specific features of crosspresenting compartments is the presence of ER-resident proteins (Ackerman et al., 2003, 2006; Guermonprez et al., 2003; Houde et al.,

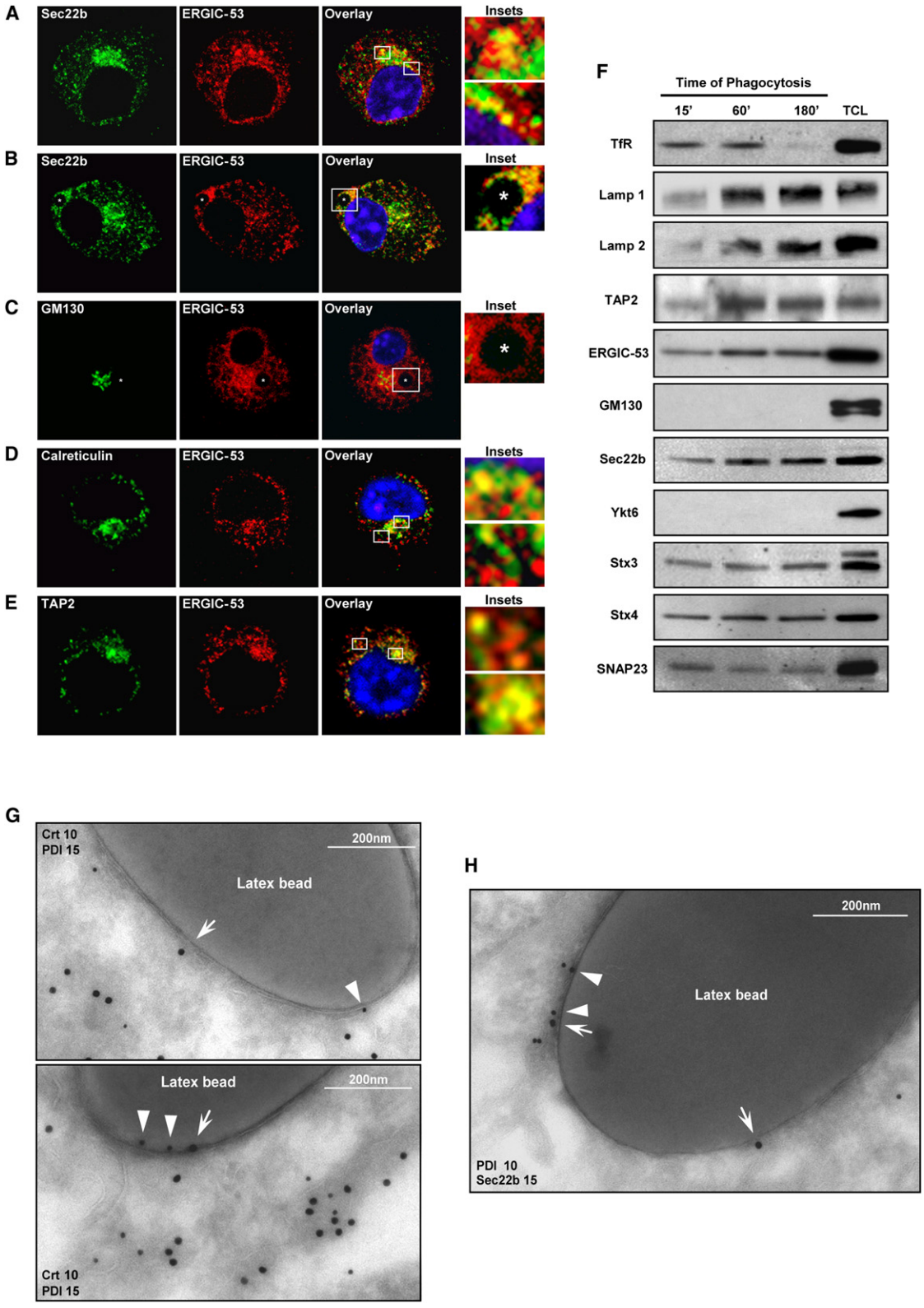

Figure 1. Sec22b Localizes to the ERGIC and Is Early and Efficiently Recruited to DC Phgs

(A–E) IF detection of ERGIC-53 (red) and (A and B) Sec22b (green), (C) GM130 (green), (D) Calreticulin (green), and (E) TAP2 (green) in (A, D, and E) BMDCs in steady state or (B and C) after 1 hr phagocytosis of LB. Asterisks indicate the LB. IF images were analyzed by confocal microscopy. Nuclei were stained with DAPI.

2003); even so, a mechanism to explain the acquisition of ER content by Phgs is still lacking.

Therefore, in order to determine the molecular mechanisms underlying the acquisition of ER proteins by Phgs in DCs, we aimed to analyze the membrane fusion machinery involved in the interaction between the two compartments. Intracellular membrane fusion requires special mechanisms for recognition (tethering) and attachment (docking), preceding actual fusion (Ungermann et al., 1998). Intracellular membrane fusion is controlled by a family of membrane and cytosolic proteins called SNAREs. The formation of *trans*-complexes linking SNAREs present in the donor and acceptor compartments provides the necessary energy for membrane mixing (Südhof and Rothman, 2009). Specific pairs of SNAREs determine the fusion of transport intermediates in all known intracellular traffic events. In macrophages, the ER-SNAREs Sec22b and syntaxin (Stx) 18 were proposed to play a role in phagocytosis (Becker et al., 2005; Hatsuzawa et al., 2000, 2006, 2009). However, the role for these SNAREs in the actual fusion between the ER and the forming Phg is still unclear.

Here, we show that Sec22b controls the recruitment of ER and ER-Golgi intermediate compartment (ERGIC) resident proteins to Phgs. The knockdown (KD) of Sec22b decreases the recruitment of different ER proteins to Phgs, causing a strong inhibition of Ag crosspresentation, but not endogenous or MHC class II-restricted Ag presentation. The KD of Sec22b also impaired the crosspresentation of Ags expressed in *T. gondii*, *E. coli*, or Ags taken up by endocytosis, suggesting that we have unraveled an intracellular traffic pathway generally required for Ag crosspresentation. We conclude that ER protein recruitment to Phgs critically influences phagosomal functions in DCs and determines Ag crosspresentation.

RESULTS

Sec22b Localizes to the ERGIC and Is Efficiently Recruited to Phgs in DCs

The recruitment of ER-resident proteins to Phgs has been reported by several groups, using both organelle isolation and immunofluorescence (IF) microscopy (reviewed in Amigorena and Savina, 2010). The interaction between the two compartments could involve either direct fusion of ER stacks to Phgs or vesicular intermediates. In both cases, a fusion event between the ER or ER-derived membrane vesicles and Phgs must occur. The SNARE Sec22b was shown to pair effectively with several plasma membrane SNAREs (McNew et al., 2000) and was proposed to influence phagocytosis in macrophages (Becker et al., 2005; Hatsuzawa et al., 2009). In order to investigate the potential role of Sec22b in ER-Phg interactions in DCs, we first analyzed its subcellular distribution using IF and confocal microscopy. As shown in Figure 1A, Sec22b labels numerous cytoplasmic structures abundant around the nucleus, as well as a more concentrated compartment displaying an asymmetric perinuclear distribution. The vesicular structures display partial colocalization with the ER marker KDEL (Figure S1A available online), and the perinuclear compartment colocalizes with the *cis*-Golgi marker GM130 (Figure S1A). The overall label obtained for Sec22b is very similar to that obtained with the ER-Golgi intermediate compartment (ERGIC) marker ERGIC-53 (Figure 1A). Many of the vesicular structures observed displayed a partial colocalization, suggesting that Sec22b and the other markers analyzed are present in different subcompartments of the same ER structures (Figure 1A, see insets). The Sec22b-positive compartments are not labeled by markers of the *trans*-Golgi (TGN46), of the recycling compartment (TfR), or of late endosomes-lysosomes (Lamp1) (Figure S1A). We conclude that, in DCs, most Sec22b accumulates in the ERGIC and *cis*-Golgi compartments.

We reasoned that, if Sec22b was somehow involved in the recruitment of ER proteins to the phagocytic pathway, it should be also present in Phgs. We first investigated this issue using IF. Indeed, upon phagocytosis by DCs, Sec22b accumulated around latex bead (LB) Phgs (Figures 1B and S1B). We also found the recruitment of ERGIC53-positive structures to Phgs that were not labeled by GM130 (Figures 1B and 1C). These results indicate that, although Sec22b colocalizes with both ERGIC and *cis*-Golgi markers, only the former is efficiently recruited to Phgs. This finding also suggests that Sec22b mediates the recruitment of ER proteins from the ERGIC, rather than from the ER itself. Indeed, ER-resident proteins such as Crt, tapasin, or TAP2 were all shown to be present in post-ER compartments, including the ERGIC in other cell types (Ghanem et al., 2010; Howe et al., 2009). As depicted in Figures 1D and 1E, the labeling of both Crt and TAP2 exhibited significant colocalization with the ERGIC, suggesting that, in DCs, ER proteins also transit to Phgs via the intermediate compartment (IC).

Because the resolution of confocal microscopy is limited and these images proved difficult to quantify, we decided to use subcellular fractionation and western blot to test the presence of these different markers in Phgs. DC-Phgs were purified at different time points after phagocytosis and analyzed by immunoblotting. As expected, the TfR (an early endosomal marker) and Lamp1/2 (late endosome-lysosome markers) disappeared and appeared, respectively, in Phgs with the expected kinetics (Figure 1F). Sec22b was also present in purified Phgs, together with other ER and ERGIC proteins, including TAP2 and ERGIC53 (Figure 1F). Another ER-SNARE, Ykt6, and the *cis*-Golgi marker GM130 were not detected in the purified Phg preparations. The plasma membrane SNAREs Stx3 and 4, as well as SNAP23, all putative Sec22b-interacting partners (McNew et al., 2000), were present in purified DC-Phgs (Figure 1F). In order to determine the putative Sec22b-interacting SNAREs, we immunoprecipitated Sec22b in steady-state BMDCs or after 1 hr of phagocytosis. As a control for the immunoprecipitation, we tested for a known partner of Sec22b in ER-to-Golgi traffic,

(F) Immunoblotting of BMDC-purified Phgs and the total cell lysates (TCL). Total protein amount corresponding to 5 μg and 25 μg was loaded for purified Phgs and TCL, respectively.

(G and H) Immunoelectron microscopy (IEM) showing (G) the recruitment of the ER-resident proteins, Crt (arrowheads), and PDI (arrows) and (H) Sec22b (arrows) and PDI (arrowheads) to 1 hr DC Phgs.

Data are representative of three independent experiments. See also Figure S1.

Stx5 (Xu et al., 2000). As expected, an interaction between Sec22b and Stx5 was detected in steady-state DCs (Figure S1C). Sec22b also coprecipitated Stx4 (Figure S1D), both after 1 hr of phagocytosis and in steady state (data not shown), indicating that, similarly to reported in other cell types (Arasaki and Roy, 2010), Stx4 interacts with Sec22b in DCs. Conversely, we were not able to detect SNAP23 (Figure S1E) or Stx3 (Figure S1F) associated to Sec22b after immunoprecipitation. As an additional control, calnexin (an abundant ER protein) was not detected (even under blotting over exposure) in the precipitates (Figure S1G), indicating that they are free of noninteracting proteins from the ER-ERGIC compartments. We conclude that Stx4, which is present in early DC-Phgs, probably as a consequence of the internalization process, would serve to pair Sec22b, which is present in the ERGIC membranes. Sec22b/Stx4 interaction allows the fusion between the two compartments. The fact that this SNARE complex is also formed in the absence of phagocytosis suggests that this membrane trafficking is constitutively active in DCs, linking the ER-ERGIC with both endocytic and phagocytic pathways.

Finally, we sought to document the presence of ER-resident molecules in the phagosomal limiting membrane using cryoimmunoelectron microscopy (IEM). As shown in Figure 1G, Crt and PDI (another ER marker) antibodies labeled the phagosomal limiting membranes in a significant number of DCs (see below). Similar results were obtained using Sec22b-specific antibodies (Figure 1H). Altogether, the results presented confirm that certain ER and ERGIC proteins, but not a *cis*-Golgi resident (GM130), are recruited to Phgs in DCs. The presence in Phgs of Sec22b and Stx4 and the observation that the two SNAREs coprecipitate suggest that the two molecules are components of the molecular machinery involved in the interactions between the two compartments.

Sec22b Is Required for the Recruitment of ER Proteins to Phgs

In order to investigate the role of Sec22b in ER-Phg interactions, we knocked down its expression in a DC-line (JAWS-II), using lentivirus-delivered short hairpin RNAs (shRNA). As shown in the immunoblot of Figure 2A, two different shRNAs inhibit Sec22b expression with different efficacies, as compared to DCs transduced with the scramble (Scr) shRNA control. The inhibition of the expression of Sec22b in DCs was also evident when the same cells were analyzed by IF (data not shown) or IEM (Figure S2A). The KD of Sec22b did not change the phenotype of these cells, nor their growth rates and viability (data not shown).

To assess the effect of Sec22b KD on the recruitment of ER-resident proteins to Phgs, we isolated Phgs from the Scr or the Sec22b KD cells (using the Sec22b #2 shRNA) and quantified the recruitment of ER components by western blot. Similar to BMDCs, Sec22b was recruited to Phgs of Scr cells, whereas Ykt6 was not (Figure 2B). The levels of Sec22b were lower in Sec22b KD cells in both purified Phgs and total lysates, as compared to Scr cells. Importantly, whereas the total levels of different ER proteins, including TAP2, tapasin, and Crt, were not affected, their recruitment to Phgs was decreased in Sec22b KD cells as compared to Scr cells (Figures 2B and S2B). The Phg maturation marker Lamp1 was recruited to Phgs with slightly faster kinetics in Sec22b KD cells, as compared to Scr cells (Figure 2B).

The recruitment of another ER marker, PDI, to Phgs in Sec22b KD and Scr cells was also quantified using IEM. In order to accurately quantify the PDI phagosomal acquisition by IEM, we first optimized the use of the antibody to obtain high levels of ER labeling (around 200 gold particles/μm^2 versus around 12 gold particles/μm^2 in previous studies; Touret et al., 2005). In both Scr and Sec22b KD DCs, the typical ER membrane structures were similarly labeled by the immunogold (Figure 2C). The PDI labeling in unrelated intracellular structures such as the mitochondria (Figure S2C), the plasma membrane, or the nucleus (data not shown) was almost negligible (only 1 gold particle/50 mitochondria) as compared to the highly significant labeling observed in the ER structures (Figure S2C). Because LB-Phgs lacks any internal membrane content (it is a plastic particle), the quantification of the immunogold labeling of Phgs was not performed using the conventional gold particles/μm^2 used for quantification of the ER and mitochondria labeling (Figure S2C) but, rather, as a percent of positive organelles. A similar analysis is shown for mitochondria (Figure 2F). In Sec22b KD DCs, the PDI labeling was strongly reduced around Phgs (less than 7% of PDI (+) Phgs), as compared to Scr DCs (34% of PDI (+) Phgs) (Figures 2D–2F). The number of gold particle per positive Phg was also reduced in Sec22b KD cells (data not shown). We conclude that, in DCs expressing lower levels of Sec22b, the recruitment of ER proteins to Phgs is impaired.

Additional functional evidence for ER-Phgs interactions came from the analysis of N-glycosylation activity (an exclusive ER property) in Phgs, using a bead assay previously described (Ackerman et al., 2006). A peptide bearing N-glycosylation sites was covalently bound to LBs. After phagocytosis by the Scr and the Sec22b KD cells, N-glycosylation of the bead-bound peptide was assayed using a fluorescent lectin. A significant reduction of glycosylation associated with the beads was observed in the Sec22b KD Phgs, as compared to that detected in Scr Phgs (Figures S2D and S2E). These results further confirm that Sec22b mediates the recruitment of ER components to DC-Phgs.

Sec22b Is Required for Ag Crosspresentation

We first analyzed the effect of Sec22b silencing in crosspresentation by using OVA-coated beads or soluble OVA and the T cell hybrid B3Z, specific for the OVA peptide (SIINFEKL), in association with Kb class I MHC molecules. For both bead-coated and soluble OVA, we found a strong inhibition of crosspresentation in Sec22b KD cells, as compared to the Scr cells (Figures 3A and 3B, respectively). As a control, both the level of MHC class I molecules at the cell surface (measured by FACS; data not shown) and the presentation of the corresponding synthetic peptide were similar in both cell types (Figure 3C), suggesting that reduced crosspresentation upon Sec22b silencing is caused by a defect in phagosomal functions rather than a deficiency in MHC class I peptide trafficking. We took advantage of the two Sec22b shRNAs that inhibited the expression of Sec22b with different efficiencies (Figure 2A) to evaluate crosspresentation and found that the degree of inhibition of OT-I OVA-specific transgenic T cell activation followed that of the inhibition of the

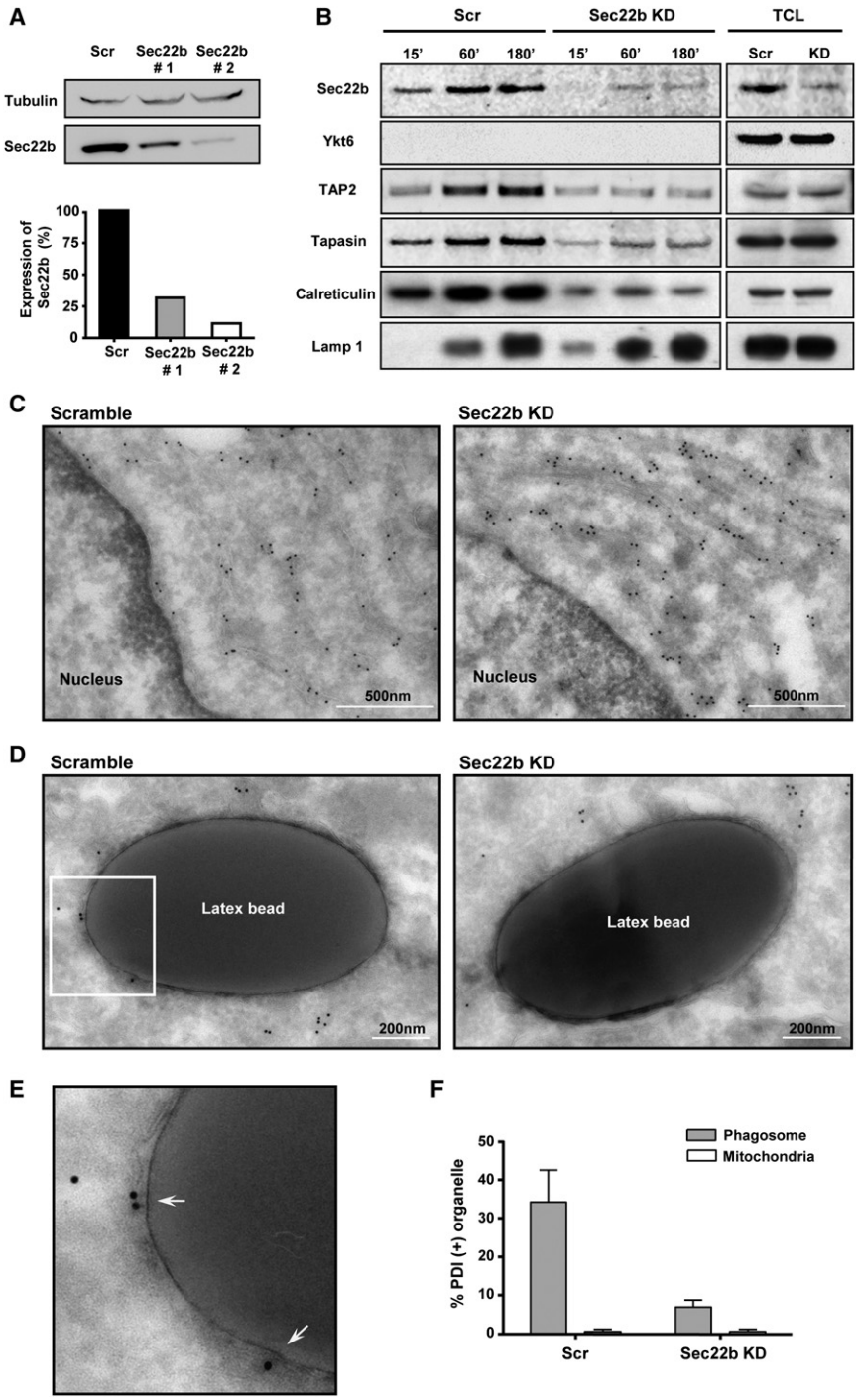

Figure 2. Sec22b Mediates the Acquisition of ER Components to DC Phgs

(A) Immunoblotting of JAWS-II cells and densitometry quantification after infection with three different lentiviruses encoding a random sequence (Scramble, Scr) and two different shRNA targeting Sec22b (Sec22b # 1 and Sec22b # 2).

(B) 5 μg of purified Phgs and 25 μg of protein of TCL from Scr and Sec22b # 2 cells (Sec22b KD) were loaded and analyzed by western blot for different proteins (one representative experiment of five).

(C and D) Immunogold labeling by EM in Scr and Sec22b KD DCs showing (C) an area close to the nucleus or (D) 1 hr LB Phgs.

(E) Inset showing magnification of the phagosomal membrane and the recruitment of PDI in Scr DCs (arrows).

(F) Quantification of PDI-positive organelles (Phg and mitochondria) from Scr and Sec22b KD cells; at least 57 Phgs and 60 mitochondria were evaluated in each case.

Data show mean ± SEM from three independent experiments. See also Figure S2.

expression levels of Sec22b KD (Figures S3A and S3B), supporting a direct role for Sec22b in crosspresentation.

The fact that Sec22 coprecipitated Stx4 in the absence of phagocytosis and that crosspresentation of soluble OVA was inhibited by Sec22b KD strongly suggests that Sec22b also plays a role in the recruitment of ER proteins to endosomes. To corroborate this hypothesis, we sought to localize Sec22b to endosomes containing fluorescent OVA after 30 min of internalization, using confocal microscopy. As shown in Figure S3C, we observed Sec22b-positive structures that also contain internalized OVA, indicating that Sec22b mediates the interaction between the compartment containing the ER proteins and the endocytic pathway.

Because Sec22b associates to both Stx4 and Stx5, we next attempted to investigate the potential role of these two SNAREs in crosspresentation. We were not able to obtain viable Stx4 KD DCs. In contrast, we did succeed to silence Stx5 in DCs (Figure S3D). Stx5 KD caused reduced class I MHC expression at the cell surface (Figure S3E) and reduced presentation of the SIINFEKL peptide to cognate OVA-specific TCR-transgenic or hybridoma CD8+ T cells (Figures S3F and S3G), suggesting that Stx5, unlike Sec22b, is required for the delivery of MHC class I molecules to the cell surface (it was therefore not possible to evaluate crosspresentation in this cell type). Ykt6, another ER-SNARE, plays a similar and sometimes redundant role to Sec22b in ER-to-Golgi transport in yeast and in mammalian cells (Zhang and Hong, 2001). Ykt6 is not present in DC-Phgs (Figures 1F and 2B), suggesting that it is not involved in crosspresentation. Indeed, the silencing of Ykt6 in DCs did not affect the expression of MHC class I at the cell surface (as measured by FACS; data not shown), the crosspresentation after OVA-bead phagocytosis, or the presentation of the control peptide

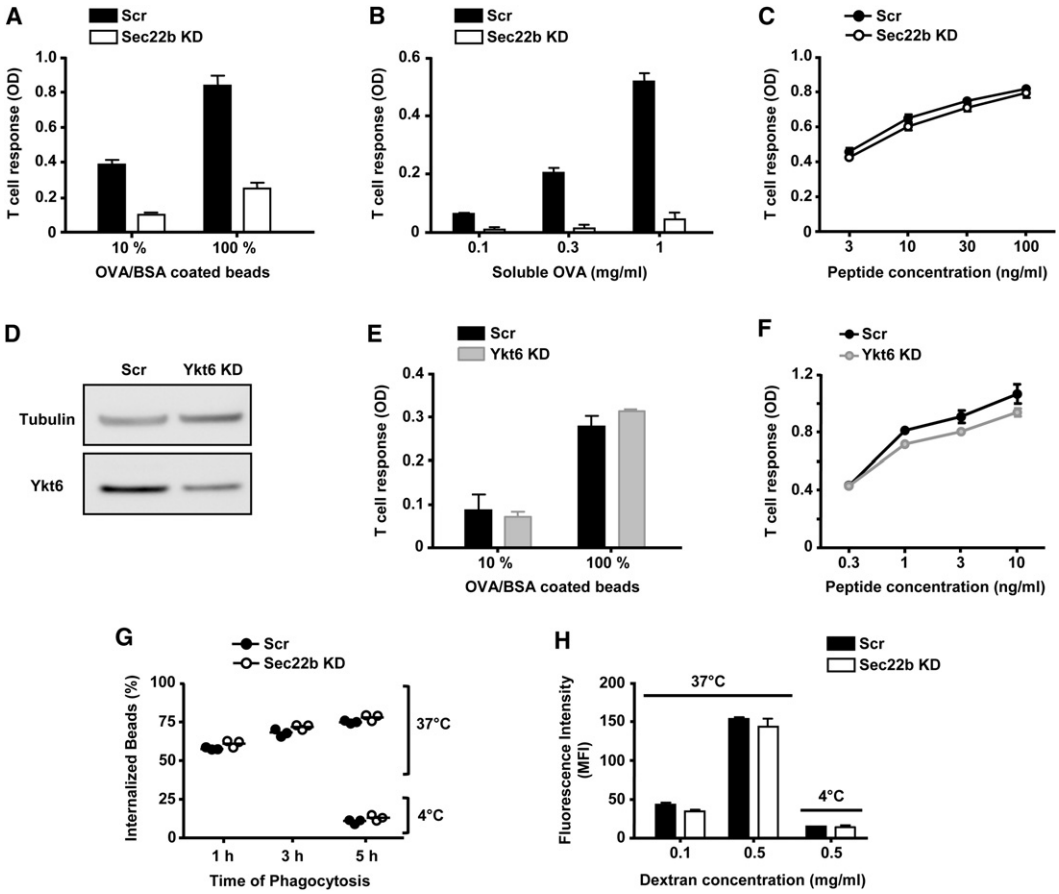

Figure 3. Sec22b KD Specifically Inhibits Crosspresentation without Affecting Ag internalization

(A–C) Crosspresentation of (A) 3μm OVA/BSA-coated beads, (B) soluble OVA, and (C) the SIINFEKL control peptide by the Src or Sec22b KD DCs was evaluated using the B3Z T cell hybridoma.

(D) Immunoblots of TCL from JAWS-II cells transduced with Scr and Ykt6 lentiviral shRNAs.

(E and F) Crosspresentations of (E) 3μm OVA/BSA-coated LBs and (F) of the corresponding synthetic peptide by Scr and Ykt6 KD DCs were evaluated by B3Z T cell hybridoma activation. See also Figure S3.

(G and H) Phagocytosis of (G) 3μm LBs and (H) endocytosis of fluorescent dextran after the indicated time periods was assessed by FACS.

Data show mean ± SEM from triplicates values and are representative of at least three independent experiments. See also Figure S4.

(Figures 3D–3F). We conclude that silencing ER-SNAREs involved in anterograde traffic (i.e., Stx5 or Ykt6) results in a phenotype that is very different from that observed upon silencing of Sec22b, indicating that the effect of Sec22b in crosspresentation is specific of this protein and independent of ER-to-Golgi traffic.

Finally, because Sec22b was proposed to regulate phagocytosis in macrophages (Becker et al., 2005; Hatsuzawa et al., 2009), we tested for a possible effect of Sec22b KD on internalization in DCs. The phagocytosis of 3 μm LBs and the endocytosis of fluorescent dextran were evaluated under the experimental conditions used in the Ag presentation assays. Neither phagocytosis nor endocytosis (Figures 3G and 3H, respectively) were affected in Sec22b KD, as compared to Scr cells (Figure S4). We conclude that, in DCs, Sec22b is dispensable for both phagocytosis and fluid phase uptake, and the observed defect in crosspresentation is due to a postengulfment event and not to reduced levels of Ag uptake.

Sec22b Is Not Required for MHC Class II and Endogenous Class I Presentation in DCs

In order to investigate whether the silencing of Sec22b expression may affect Ag presentation pathways other than crosspresentation, we transduced BMDCs with both Scr and Sec22b shRNA lentivirus (Figure 4A). Transduced BMDCs displayed a typical immature BMDC phenotype both in terms of morphology and surface markers (data not shown). Scr and Sec22b KD cells were incubated with OVA-coated beads and were assayed in parallel for MHC class II-restricted presentation to CD4+ T cells and crosspresentation to CD8+ T cells, using OT-II and OT-I anti-OVA transgenic T cells, respectively. As shown in Figure 4B, crosspresentation to OT-I cells was inhibited by 50%–60% in the Sec22b KD DCs as compared to Scr DCs, whereas presentation of the specific synthetic peptide was unaffected (Figure 4D). In contrast, the presentation of bead-bound, control peptide or soluble OVA to OT-II CD4+ T cells was unaffected by the KD of Sec22b (Figures 4C, 4E, and S5A, respectively). We

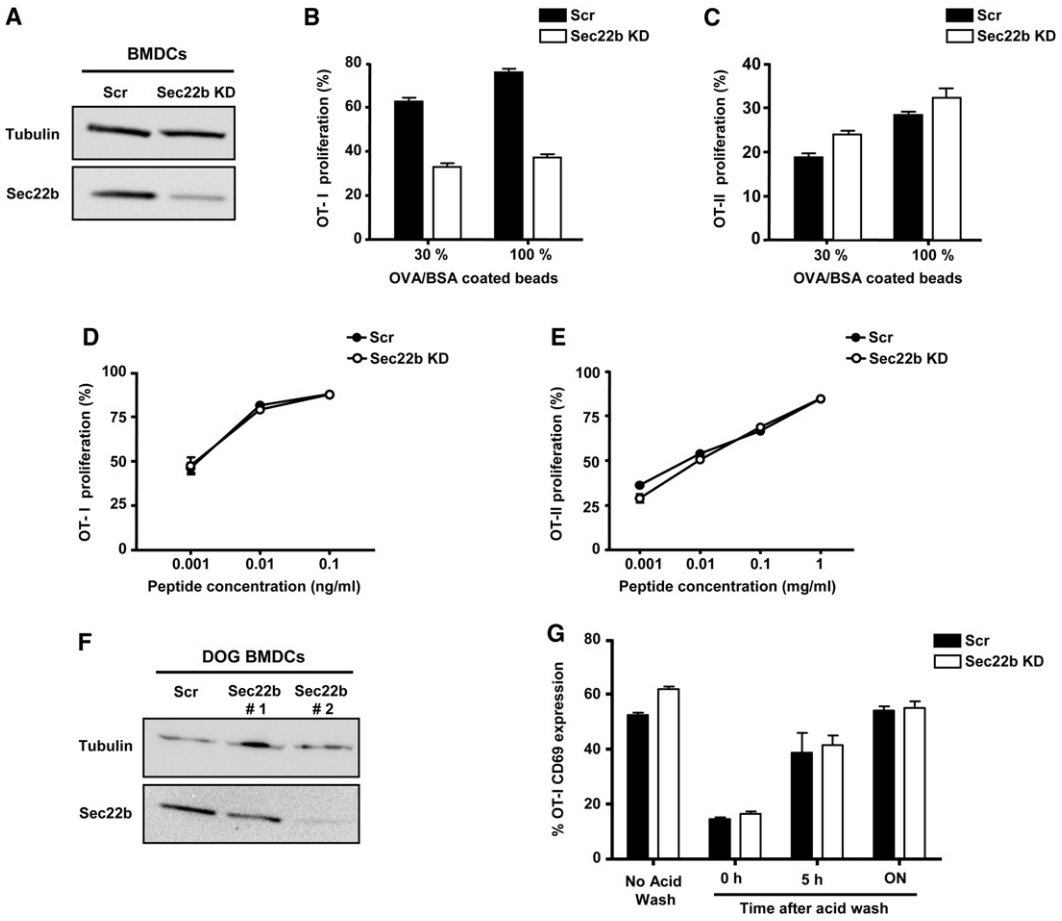

Figure 4. MHC Class II Presentation and Endogenous MHC Class I Presentation Are Not Affected by Sec22b Silencing in BMDCs

(A) Immunoblotting of TCL from BMDCs transduced with Scr and Sec22b #2 (Sec22b KD) lentiviral shRNAs.

(B–E) Transduced BMDCs were fed with 3 μm OVA/BSA-coated beads or with control synthetic peptides and were subsequently incubated with (B and D) CD8+ OT-I T cells or with (C and E) CD4+ OT-II T cells to evaluate T cell proliferation.

(F) Immunoblotting of TCL from DOG BMDCs transduced with Scr and Sec22b lentiviral shRNAs.

(G) Transduced DOG BMDCs underwent acid wash, were fixed after the indicated time points, and were subsequently incubated with OT-I T cells. OT-I activation corresponding to 5×10^4 DCs are shown.

Data show mean ± SEM from triplicate values and are representative of three independent experiments. See also Figure S5.

conclude that Sec22b silencing inhibits Ag crosspresentation without affecting MHC class II-restricted presentation to CD4+ T cells.

The presentation of endogenous Ags on MHC class I molecules requires transport from the ER to the Golgi apparatus and then to the plasma membrane. The results depicted in Figure 3 suggest that the silencing of Sec22b does not affect ER-to-Golgi traffic. To further address this issue, we tested the effect of Sec22b silencing on class I MHC-restricted presentation of endogenous Ags. BMDCs from DOG mice, which constitutively express cytosolic OVA under the control of the CD11c promoter (Hochweller et al., 2008), were transduced with Src or Sec22b shRNAs (Figure 4F). After acid wash (to eliminate the constitutively presented OVA peptides from surface MHC I molecules), OT-I T cell activation was followed over time to detect the delivery of newly formed class I MHC-OVA peptide complexes at the cell surface (Figure S5B). No difference was observed in the kinetics of OT-I T cell activation between Scr and the Sec22b KD BMDCs at any time point (Figure 4G). Therefore, the presentation of endogenous OVA by class I MHC molecules in DCs is not affected by the KD of Sec22b. Importantly, these results also indicate that the normal anterograde transport (ER-Golgi-plasma membrane) in the Sec22b KD cells is fully functional.

Crosspresentation of *Toxoplasma gondii*- and *Escherichia coli*-Derived Ags Is Compromised in Sec22b KD DCs

The involvement of the ER was shown to be important for the crosspresentation of *T. gondii*-derived Ags to CD8+ T cells (Blanchard et al., 2008). More recently, it was proposed that, in fact, the active recruitment of ER membranes to this parasite vacuole (PV) was required for efficient parasite crosspresentation (Goldszmid et al., 2009). We therefore hypothesized that

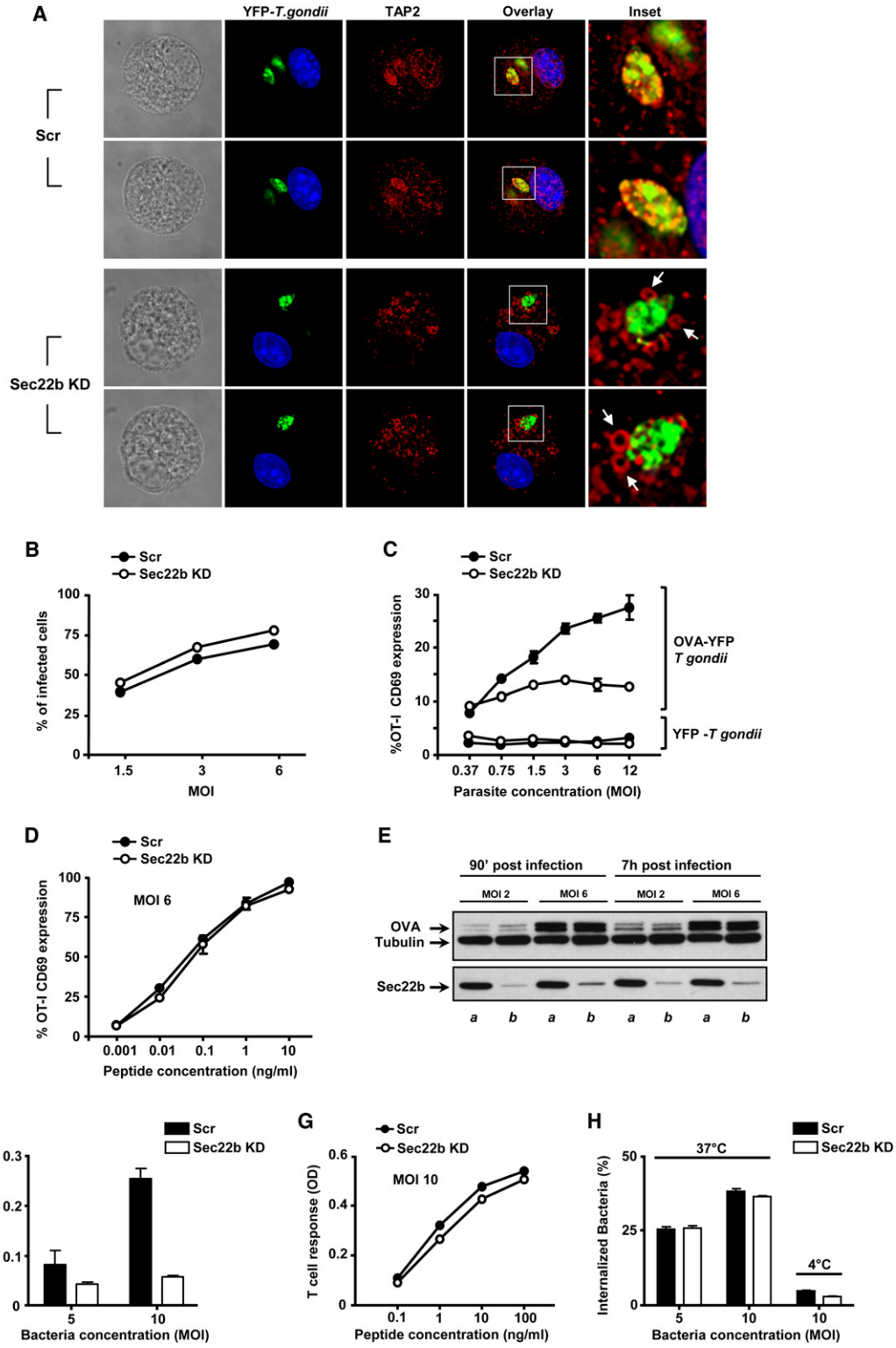

Figure 5. Sec22b Specifically Controls the ER Proteins' Acquisition by *Toxoplasma gondii* Vacuoles and the MHC Class I Presentation of *T. gondii*- and *Escherichia coli*-Associated Ags

(A) IF detection of TAP2 in transduced DCs after infection (8 hr) with OVA-YFP-*T. gondii.* Two different planes of each cell type are shown.

(B) The efficiency of infection (5 hr) of YFP-*T. gondii* in Scr and Sec22b KD cells was measured by FACS at the indicated multiplicity of infection (MOI). See also Figure S6.

the mechanisms governing ER-derived membrane delivery to latex bead Phgs in DCs may also account for the recruitment of ER components to the *T. gondii*-containing vacuole. To determine the effect of Sec22b KD in the ER recruitment to the PV, Scr and Sec22b KD DCs were infected with YFP-expressing parasites, and the distribution of the ER protein TAP2 was analyzed by IF. TAP2 was efficiently recruited to the PV in Scr DCs (Figures 5A, top, and S6A). In Sec22b KD cells, in contrast, a strong reduction of TAP2 recruitment to the PV was observed (Figures 5A, bottom, and S6B) (>90% of the PV were visibly labeled with TAP2 in Scr cells, against <30% in Sec22b KD cells; at least 50 PV were analyzed in each case). Interestingly, in Sec22b KD DCs, the TAP2-positive vesicles in close vicinity to the PV displayed a large ring shape (Figures 5A, bottom, and S6B, arrows in the insets). This observation suggests that, when Sec22b expression is decreased, TAP2-positive compartments are efficiently recruited near the PV, but the final fusion event between the two compartments is impaired. This blockage in the fusion could cause the homotypic fusion of the incoming ER-derived vesicles (actively enhanced by the parasite) and their consequent enlargement due to membrane accumulation.

In order to assess the actual role of the ER proteins in the *T. gondii* PV in Ag crosspresentation, we first evaluate parasite infection. Both cell types were similarly infected at different parasite MOI (Figure 5B). Concomitantly, GRA-2, a protein secreted by active infective parasites into the PV (Sibley et al., 1995), was clearly detected by IF in all parasite-containing compartments in both DCs types (Figure S6C). To measure crosspresentation, the Scr and Sec22b KD DCs were fixed after 8 hr of infection by OVA-expressing *T. gondii* (OVA is secreted into the vacuole; Gubbels et al., 2005) and incubated with OT-I cells. OT-I cell activation was inhibited in Sec22b KD cells, as compared to Src (Figure 5C). However, both cell types activated similarly T cells after infection with an OVA-negative parasite control and incubation with the MHC class I peptide (Figure 5D). Western blot for OVA of infected DCs showed that Sec22b KD and Scr DCs contain similar amounts of the parasite-expressed Ag (Figure 5E). We conclude that Sec22b plays a critical role in the recruitment of ER components to the *T. gondii* PV that is required for the crosspresentation of parasite-associated Ag.

Contrary to *T. gondii*, which may actively recruit ER to its PV, other types of microbes, such as *E. coli*, are internalized by phagocytes in the absence of active microbe-driven ER recruitment to their Phgs. We explored whether the contribution of ER-derived membranes to the phagocytic pathway is also important for *E. coli*-associated Ag crosspresentation by DCs. As shown in Figure 5F, a strong decrease of T cell activation was observed by Sec22b KD DCs, as compared to Scr DCs after bacterial infection. The presentation of the control OVA peptide was similar in both cell types after the same time of infection (Figure 5G), and both DC types internalized the bacteria with similar efficacies (Figure 5H). We conclude that, independently of active ER recruitment by the pathogen, Sec22b is required for the efficient crosspresentation of phagocytosed Ags expressed in *E. coli*.

Sec22b Is Required for Ag Export to the Cytosol in DCs

Several roles were proposed in the past for ER-resident proteins present in Phgs, including Ag export from Phgs and endosomes to the cytosol (Ackerman et al., 2006; Lin et al., 2008). Export to the cytosol was quantified using two different approaches. The first one is based on the toxicity of cytochrome C (cytC) when present in the cytosol (Lin et al., 2008). After feeding the DCs with cytC, apoptosis (detected by annexin V labeling) was used as a measure of the delivery of endocytosed cytC to the cytosol (Figure S7A). As shown in Figures 6A and S7B, the labeling of DCs with annexin V is significantly decreased in Sec22b KD, as compared to Scr cells. The second assay for the cytosolic export was modified from a method previously used to measure the rupture of bacterial Phgs (Ray et al., 2010). DCs were loaded with a FRET substrate of β-lactamase (CCF4), which accumulates in the cytosol. The cells are then fed with β-lactamase, which upon export to the cytosol, cleaves its substrate CCF4, resulting in a loss of FRET signal at 535 nm and an increased emission at 450 nm (Figure S7C). By calculating ratiometric values between both signals (450:535) by FACS, we can measure β-lactamase export to the cytosol in real time, which results in an increase of the ratiometric measurement. As shown in Figure 6B, the ratio values are significantly smaller in Sec22b KD cells compared to the Scr, indicating reduced export of the β-lactamase to the cytosol. Fluorescence microscopy analysis confirmed these results, as shown in Figures 6C and 6D. As a control, the amount of β-lactamase internalized by the two cell types was similar, as evaluated by FACS after 90 min of endocytosis of a fluorescent version (Figure 6E) or by enzymatic activity measurement of the total cell lysate after different times of internalization (Figure 6F). These data respectively indicate that the variation observed in the ratiometric values was not due to any defect in β-lactamase internalization or enzymatic inactivation after endocytosis. We concluded from these two series of experiments that the recruitment of ER-resident proteins to the endocytic pathway is required for efficient export of internalized cargo to the cytosol.

(C) Crosspresentation of OVA secreted by *T. gondii* (OVA-YFP-*T. gondii*) or control *T. gondii* (YFP-*T. gondii*) after 8 hr of infection at indicated MOI was evaluated by OT-I cell activation.

(D) Transduced DCs were infected with control *T. gondii* (8 hr at MOI 6) and incubated with the control synthetic peptide; after fixation, OT-I cell activation was evaluated.

(E) Immunoblotting showing the total amount of OVA in (a) Scr and (b) Sec22b KD DCs after 90 min and 7 hr of infection with OVA-YFP-*T. gondii* at two different MOI.

(F) Crosspresentation of OVA-expressing *E. coli* after 5 hr of internalization by the Scr and Sec22b KD cells at two different MOI was assayed by B3Z T cell hybridoma activation.

(G) The control peptide curve was performed by infecting DCs with control *E. coli* (not expressing OVA) at MOI 10 during 5 hr.

(H) The internalization capacity of *E. coli* by Scr and Sec22b DCs was evaluated by FACS by using CFSE-labeled bacteria.

Data show mean ± SEM from triplicate values and are representative of at least three independent experiments.

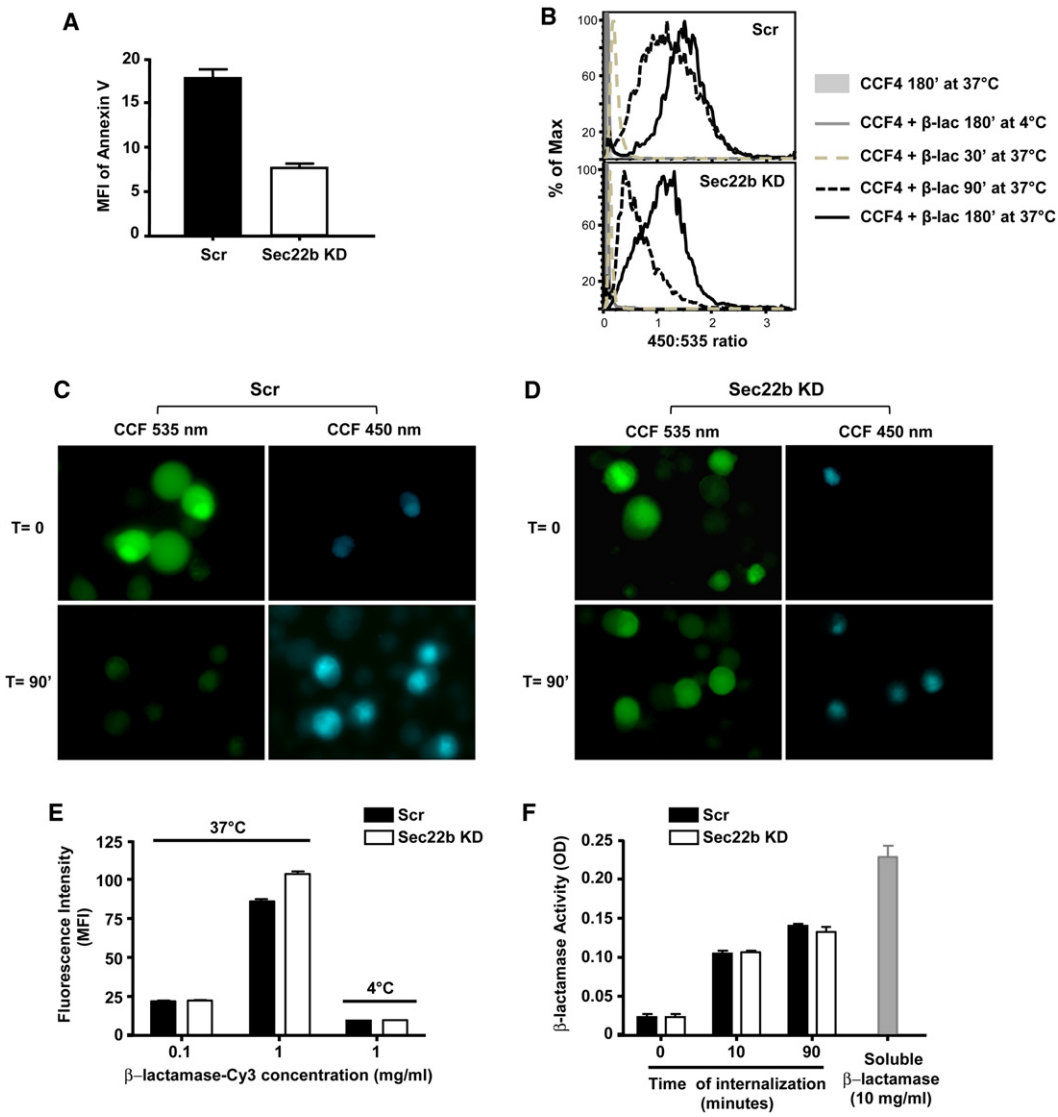

Figure 6. Sec22b-Mediated Contribution of the ER Components to the Internalization Pathway Is Critical for Ag Export to the Cytosol

(A) Endosome-cytosol export was evaluated by measuring annexin V labeling in cells by FACS after internalization of exogenously added cytC. Data show mean ± SEM from triplicate values and are representative of three independent experiments.

(B) The histograms represent the ratiometric values (450:535) obtained by FACS analysis.

(C and D) CCF4-loaded DCs were fed during 90 min with β-lactamase and observed on wide-field epifluorescence microscope at 40× magnification. 405 nm wavelength was used for excitation of CCF4. Emission at 535 nm (FRET green/intact probe) and 450 nm (deFRET blue/cleaved probe) were analyzed in (C) Scr and (D) Sec22b KD DCs.

(E) Endocytosis (90 min) of fluorescent β-lactamase at two different concentrations was evaluated by FACS.

(F) Total enzymatic activity after internalization of 2 mg/ml of β-lactamase in Scr and Sec22b KD DCs was analyzed by spectrophotometry using an enzymatic test.

(B–D) Results are representative of three independent experiments. (E and F) Data show mean ± SEM from triplicate values and are representative of two independent experiments. See also Figure S7.

The Recruitment of ER Components to Phgs Delays Phagosomal Maturation

Although it is still difficult to estimate the proportion of ER-derived proteins and membrane that is actually delivered to Phgs, we reasoned that the presence of ER-derived material may modify Phg maturation. We first analyzed phagosomal degradation in individual Phgs using FACS analysis (phagoFACS) (Savina et al., 2010). The kinetics and efficiency of phagosomal OVA degradation were much faster in DCs KD for Sec22b (Figure 7A). Enhanced protein degradation correlates with an increased phagosomal acquisition of the lysosomal marker Lamp1, as quantified by western blot in Sec22b KD-purified Phgs (Figures 7B and 2B). The amount of cathepsin (Cath) D (mature form) in Sec22b KD Phgs was increased (whereas the ER protein,

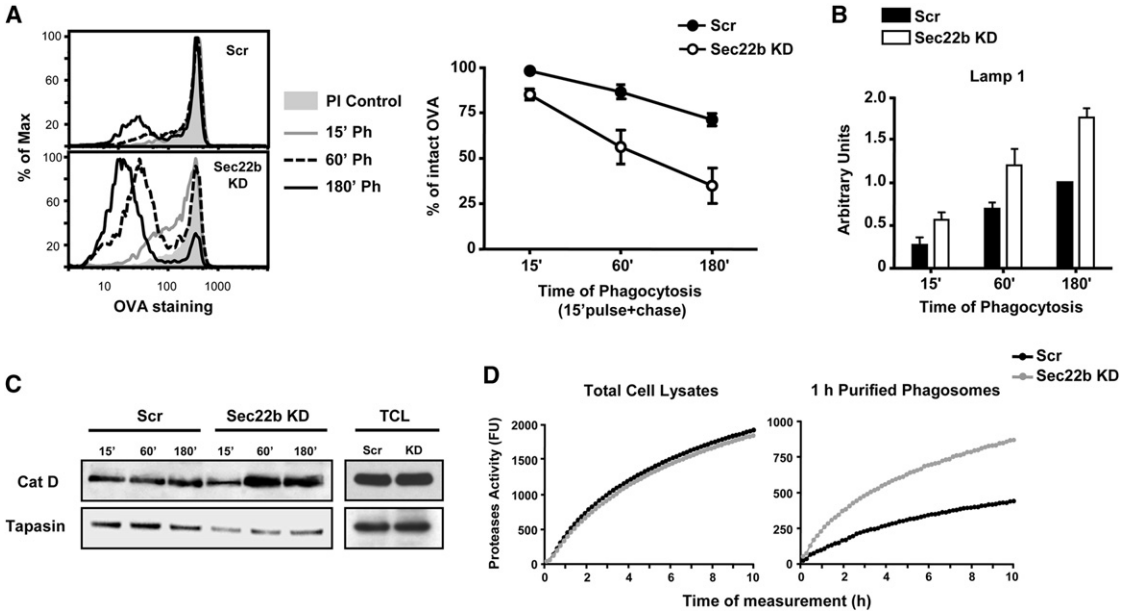

Figure 7. Acquisition of ER Components by Phgs Modulates Phagosomal Maturation and Proteolysis in DCs

(A) Intact OVA staining on isolated Phgs was measured by FACS at indicated time periods. (Left) Typical phago-FACS profiles from one representative experiment (PI, protease inhibitor control). The kinetics of OVA degradation (as percentage of proteases inhibitors) in Phgs from Src and Sec22b KD DCs are shown in the right panel. Data show mean ± SEM of three independent experiments.

(B) Densitometry quantification ± SEM for the lysosomal marker Lamp1 immunoblots from five independent Phg purifications.

(C) Purified Phgs from Scr and Sec22b KD cells were analyzed by immunoblotting for Cath D and tapasin. Data are representative of three independent Phg purifications. See also Figure S8.

(D) TCL and 1 hr purified Phgs were incubated with a mixture of different fluorogenic substrates of Cath B–L, H, G, and asparagine endopeptidase (AEP). Proteases activity was assayed at pH 7.4 over time. Results are expressed as fluorescence units (FU). Data are representative of three independent experiments.

tapasin, was decreased), as compared to Phgs from Src DCs (Figure 7C). Interestingly, the levels of the immature form of Cath D are lower in Sec22b KD Phgs compared to Scr Phgs (Figure S8). Because the processing of pro-Cath D is dependent on the proteolytic activity of other cathepsins, such as Cath L and B (Laurent-Matha et al., 2006), this finding validates that phagosomal environment becomes more proteolytic in Sec22b KD DCs. Likewise, the proteolytic activity in purified Phgs from Sec22b KD DCs, as measured using synthetic fluorescent substrates specific for several proteases (asparagine endopeptidase [AEP], cathepsins B-L, H, and G) at fixed pH (7.4, the actual phagosomal pH in both DC types; data not shown), was higher in Phgs from Sec22b KD cells (Figure 7D), indicating that there is a high number of these proteases present in Phgs devoid of ER components. We conclude that Sec22b-dependent acquisition of ER-derived membranes by Phgs delays phagosomal maturation in DCs.

DISCUSSION

The model originally proposed in macrophages by which the ER stacks can directly fuse with forming phagosomes, generating a mix phagosome-ER compartment (Gagnon et al., 2002), led us to hypothesize a mechanism by which ER proteins were recruited to phagosomes for crosspresentation in DCs. Both the model for ER protein recruitment to phagosomes and the functional relevance of this process were questioned and remained controversial (Touret et al., 2005). This debate has grown, at least in part, due to the lack of definition of a transport pathway linking the two compartments. The identification of Sec22b as a critical component of the molecular machinery involved in ER-to-Phg traffic in DCs establishes the existence of a membrane transport pathway. By blocking the interaction between the two compartments, we addressed the functional role of the contribution of ER-resident proteins to Phgs. We demonstrate that reducing the levels of ER proteins in DC-Phgs has three main functional consequences: deficient crosspresentation, reduced Ag export to the cytosol, and accelerated lysosomal fusion and increased protein degradation in Phgs.

Our results show that, in DCs, Sec22b mainly colocalizes to markers of the intermediate compartment (ERGIC-53) and the *cis*-Golgi (GM130), within a concentrated perinuclear population of tubules and vesicles. Importantly, by using both subcellular fractionation and IF, we found that only ERGIC-53 is recruited to Phgs, whereas GM130 is not (Figure 1), suggesting a direct interaction between Phgs and the ERGIC in DCs. What then is the role of ERGIC in ER-Golgi trafficking in DCs? The identity and function of this compartment located between the ER and the Golgi starts to be understood in mammalian cells. Increasing evidence indicates that the ERGIC is a mobile structure of small vesicles that carry secretory material between the ER exit sites (ERES) and the Golgi complex while constantly maturing, segregating, and returning material to the ER (reviewed in Appenzeller-Herzog and Hauri, 2006). Interestingly, we observed that, in DCs,

the ER-resident Crt and TAP2 are present in the IC (Figures 1D and 1E). Therefore, we propose that proteins of the class I MHC-loading machinery transit from the ER to the ERGIC, where they are sorted and either returned to the ER or directed through a Secc22b-dependent mechanism to the phagosomal compartment.

Our findings also demonstrate that the role of Sec22b in cross-presentation is not restricted to LBs and soluble OVA. In two different microbial models (*E. coli* and *T. gondii*), crosspresentation was severely impaired in the Sec22b KD cells. Interestingly, these two pathogens enter DCs through completely different pathways. *E. coli* is phagocytosed into conventional Phgs and was not described to actively interfere with the phagocytic process. *T. gondii*, in contrast, invades cells using a PV, a structure that is very different from a Phg. We now show that the massive recruitment of ER proteins to the *T. gondii* PV and the crosspresentation of Ags expressed by the parasite are both lost in the absence of Sec22b. Together, these results indicate that, in DCs, Sec22b controls a general pathway of membrane traffic that links the ER to various structures containing extracellular material (Phgs and endosomes).

One of the main functions of this Sec22b-dependent ER-to-Phg pathway is related to crosspresentation. Why then is the recruitment of ER components to Phgs important for crosspresentation? It is most likely that there is not a unique response to this question. On the one hand, ER proteins that are present in Phgs were proposed to play different roles during crosspresentation. TAP1/2 was shown to mediate the import of eight to nine amino acids into Phgs, allowing the loading of class I MHC molecules within Phgs (Guermonprez et al., 2003; Houde et al., 2003). The ER retrotranslocation machinery, including the p97 ATPase, was proposed to mediate export of phagosomal cargo into the cytosol (Ackerman et al., 2006). This proposal is consistent with our observation that export from endosomes to the cytosol is defective in Sec22b KD cells (Figure 6). On the other hand, we also show that phagosomal degradation is boosted in the Sec22b KD cells, which we showed previously also impairs crosspresentation. We therefore suggest that the recruitment of ER proteins to Phgs favors crosspresentation in several ways. First, it promotes the Ag export to the cytosol; the import of the processed peptides back into the Phgs; and the loading of the peptides on class I MHC molecules (through the peptide loading complex). Second, we show here that the phagosomal acquisition of ER-ERGIC components delays the recruitment of lysosomal content, defining an unexpected mode of modulation of phagosomal maturation. This observation suggests that ER membranes bear molecules (lipids or proteins) that actively inhibit lysosomal fusion. Indeed, in Sec22b-deficient DCs, the recruitment of the lysosome marker Lamp1 and of proteases such as Cath D is accelerated in ERGIC-deprived Phgs, resulting in enhanced proteolytic degradation of phagosomal cargo (Figure 7). Because there is important evidence that increased proteolytic activity in Phgs is detrimental for crosspresentation (Savina et al., 2006, 2009), the modulation of phagosomal maturation through the acquisition of ER components most likely represents an adaptation of DC's endophagocytic pathway for crosspresentation.

The effect of the ER/ERGIC-Phg interactions on lysosome-Phg fusion may have an impact beyond Ag crosspresentation. Interestingly, such a functional interaction between the ER/ERGIC and Phgs is important for the pathogenicity of many microbes, including *Legionella*, *Brucella*, or *Toxoplasma*, which have evolved to actively target this ER-Phg pathway as a survival strategy (Celli et al., 2003; Kagan et al., 2005; Melo and de Souza, 1997). In the particular case of macrophage infection by *Legionella*, it has been shown that, once internalized, this pathogen actively recruits ERGIC membranes through a Sec22b-dependent mechanism (Kagan et al., 2005; Machner and Isberg, 2006). Surprisingly, our results showing that, in DCs, ERGIC is recruited to Phgs in the absence of an active microbial signal further suggest that *Legionella* may have hijacked and exacerbated an existing ER-related mechanism of inhibition of lysosomal fusion for its benefit, rather than generate a new traffic event. Thus, our finding that ER/ERGIC contribution to phagosomes delays fusion to lysosomes is consistent with the notion that microbes exploit this membrane traffic pathway to avoid degradation in lysosomes. On the other hand, it may imply that, as host cells, DCs respond in turn by making these pathogens visible to the immune system through crosspresentation.

EXPERIMENTAL PROCEDURES

Mice and Cells

For full information on mice and cells, see Extended Experimental Procedures.

Lentiviral shRNA Knockdown of Sec22b, Ykt6, and Stx5

The generation of lentivirus was done by using plasmids encoding lentiviruses expressing shRNAs obtained from the library of The RNAi Consortium (TRC) and by transfection into HEK293T cells, as has been previously detailed (Moffat et al., 2006). DC infection was performed as described before (Savina et al., 2009). For detailed information about the protocol and the shRNA target sequences, see the Extended Experimental Procedures.

Phagosome Purification

BMDCs and JAWS-II cells were incubated with 3 μm magnetic beads for 20 min at 18°C and 15 min at 37°C in incomplete CO_2-independent medium (pulse), and after extensive washes with cold 0.1% PBS/BSA, the cells were incubated at 37°C for the indicated times with complete medium. Cells were then disrupted in homogenization buffer (PBS 8% sucrose, 3 mM imidazole, 2 mM DTT, 5 μg/ml DNase, and 2 × protease inhibitor cocktail), as described previously (Guermonprez et al., 2003). Magnetic Phgs were removed from the postnuclear supernatant using a magnet, centrifuged once in 1 ml of serum, and washed three times in cold washing solution (10 mM HEPES, 110 mM KCl, 10 mM NaCl, 5 mM $MgCl_2$, and 2 mM DTT in H_2O). Phgs were then lysed in lysis buffer (RIPA buffer plus 2 mM DTT and 1 × protease inhibitor cocktail) during 30 min at 4°C, and cellular debris were excluded from the solution by centrifuging 5 min at 15,000 rpm.

Electron Microscopy

Scr and Sec22b KD DCs were fed with 1 μm LBs during 1 hr (30 min pulse + 30 min chase) at 37°C. Cells were extensively washed and fixed in 4% PFA (in 0.1 M Phosphate Buffer) during 2 hr at room temperature. IEM was performed by the Tokuyasu method (Slot and Geuze, 2007). Single- or double-immunogold labeling on ultrathin cryosections was performed using protein A-gold conjugates (PAG) (Utrecht University, The Netherlands). The following antibodies were used at the indicated dilutions: anti-PDI (1:250), anti-Crt (1:50), and/or rabbit polyclonal anti-Sec22b (1:100). Sections were examined using a Tecnai 12 electron microscope (FEI Company) equipped with a digital camera Keen View (SIS). Quantification of gold particles/ μm^2 was done using iTEM analySIS software (Soft Imaging Systems).

Ag Presentation Assays

Crosspresentation and MHC Class II Presentation

BMDCs were incubated with 3 μm OVA-coated LBs or with different concentrations of the control minimal peptides (OVA SIINFEKL or OVA 323–339). After 1 hr, DCs were washed and cocultured with purified CFSE-OT-1 $CD8^+$ or purified CFSE-OT-2 $CD4^+$ T cells for 3 days. To evaluate T cell proliferation, diminution of CFSE staining on TCR^+ $CD8^+$ and $CD4^+$ populations was measured by FACS. Alternatively, JAWS-II cells were incubated for 5 hr with soluble OVA, OVA-coated beads, or the SIINFEKL peptide. After this time, cells were washed and fixed with 1% PFA, and B3Z hybrid T cells were added. T cell activation was measured detecting β-galactosidase activity by optical density at 590 nm using CPRG as substrate for the reaction. Crosspresentation experiments were also performed with 1 μm LBs, as described in Figure S3.

Endogenous MHC Class I Presentation

BMDCs from DOG mice were transduced with Scr and Sec22b shRNAs. Cells were collected at different time points and treated with citric acid (pH 3.4) at 4°C for 2 min (Sugawara et al., 1987). After acid treatment, cells were washed extensively, and half of the cells were fixed with 0.008% glutaraldehyde. Fixed cells were then incubated with purified $CD8^+$ OT-1 cells to measure CD69 expression by FACS. In parallel, the nonfixed cells (after acid treatment) were incubated to evaluate DCs' viability by alamar blue reaction. The condition without acid treatment was also performed in both measurements. The OT-I activation (CD69% expression) was normalized to 5×10^4 DCs.

Crosspresentation of Bacteria-Associated OVA: Escherichia coli

DH5-α-expressing OVA and the control strains were used to evaluate crosspresentation capacity of DCs. After the expression of OVA was induced upon IPTG stimulation, cells were infected with both *E. coli* strains at different MOI. Then DCs were fixed with 1% PFA, and B3Z hybrid T cells were added to measure T cell activation. See a detailed version in the Extended Experimental Procedures.

Toxoplasma gondii Infection and MHC Class I Ag Presentation

YFP-RH parasites expressing OVA or not were irradiated and added to Scr and Sec22b KD DCs at various MOI. After 8 hr of infection, DCs were washed and fixed with 0.008% glutaraldehyde. Fixed cells were incubated with purified $CD8^+$ OT-1 cells, and the percentage of CD69 expression was analyzed by FACS. Alternatively, 5 hr after parasite infection, the percentage of YFP (+) JAWS-II cells at different MOI were analyzed by FACS. See also the Extended Experimental Procedures.

β-Lactamase Experiments

DCs were loaded with 1 μM of the CCF4-probe sensitive to FRET measurements during 1 hr. Then cells were washed and incubated at 37°C with 2 mg/ml of purified β-lactamase for the indicated time points. Live single cells were gated, and the fluorescence intensities of cleaved and uncleaved CCF4 were detected with the 405 nm excitation laser and 450 nm and 535 nm emission filters by flow cytometry. The histograms represent the fluorescence intensity ratio between 450/535nm emission filters. Alternatively, β-lactamase export to cytosol was analyzed by microscopy. For this, DCs were incubated with CCF4 cytosolic probe and fixed (T0 min) or loaded with 2 mg/ml of β-lactamase for 90 min (T90 min) at 37°C before fixation. To evaluate the uptake of β-lactamase and total cell enzymatic activity, DCs were subjected to nitrocefin enzymatic test and measured by spectrophotometry. For more details, see the Extended Experimental Procedures.

SUPPLEMENTAL INFORMATION

Supplemental Information includes Extended Experimental Procedures, eight figures, and two movies and can be found with this article online at doi:10.1016/j.cell.2011.11.021.

ACKNOWLEDGMENTS

We are grateful to Boris Striepen (U. of Georgia, Athens, GA, USA) and Marc-Jan Gubbels (Boston College, Chestnut Hill, MA, USA) for the gift of YFP- and OVA/YFP-expressing RH parasites and Marie-France Cesbron-Delauw for the anti-GRA2 antibody. We thank Thierry Galli (Institut Jacques Monod) for the gift of Ykt6 and SNAP-23 antibodies and for helpful discussions and comment on the manuscript. Maria Rescigno (European Institute of Oncology, Milan) for the gift of OVA-expressing *E. coli* strains. We thank Philippe Benaroch for helpful discussion about the protocol of export to the cytosol with β-lactamase; A.-M. Lennon and F. Kotsias for comments on the manuscript; and Michel Desjardins for helpful discussions. We thank Patricia Le Baccon for assistance with Delta Vision system and Christine Sedlik for technical assistance with *T. gondii* experiments. We thank the PICT-IBiSA@BDD (UMR3215/U934) Imaging facility of Institut Curie. This work was financed by Institut Curie, Institut National de la Santé et de la Recherche Médicale (INSERM), ARC (Association de la Recherche contre le Cancer, N° SFI20101201629), Ligue National de Lutte contre le Cancer (Ligue labélisée 2007-2010 and 2011-2013), European Research Council (PhagoDC n°233062), Agence National de Recherche (ANR MIME APAT), and the Bettencourt-Schueller Foundation (FBS). I.C. was supported by the Curie Institute PhD Scholarship program and the ARC. N.B. was supported by the Human Frontier Science Program Organization, INSERM, and FBS. L.F.M. receives support from Fundação Luso-Americana para o Desenvolvimento and Fundação para a Ciência e a Tecnologia (PTDC/SAU-IMU/110303/2009, PTDC/SAU-MII/100780/2008, and PIC/IC/82991/2007).

Received: May 17, 2011
Revised: September 7, 2011
Accepted: November 10, 2011
Published: December 8, 2011

REFERENCES

Ackerman, A.L., Kyritsis, C., Tampé, R., and Cresswell, P. (2003). Early phagosomes in dendritic cells form a cellular compartment sufficient for cross presentation of exogenous antigens. Proc. Natl. Acad. Sci. USA *100*, 12889–12894.

Ackerman, A.L., Giodini, A., and Cresswell, P. (2006). A role for the endoplasmic reticulum protein retrotranslocation machinery during crosspresentation by dendritic cells. Immunity *25*, 607–617.

Amigorena, S., and Savina, A. (2010). Intracellular mechanisms of antigen cross presentation in dendritic cells. Curr. Opin. Immunol. *22*, 109–117.

Appenzeller-Herzog, C., and Hauri, H.P. (2006). The ER-Golgi intermediate compartment (ERGIC): in search of its identity and function. J. Cell Sci. *119*, 2173–2183.

Arasaki, K., and Roy, C.R. (2010). Legionella pneumophila promotes functional interactions between plasma membrane syntaxins and Sec22b. Traffic *11*, 587–600.

Becker, T., Volchuk, A., and Rothman, J.E. (2005). Differential use of endoplasmic reticulum membrane for phagocytosis in J774 macrophages. Proc. Natl. Acad. Sci. USA *102*, 4022–4026.

Blanchard, N., Gonzalez, F., Schaeffer, M., Joncker, N.T., Cheng, T., Shastri, A.J., Robey, E.A., and Shastri, N. (2008). Immunodominant, protective response to the parasite Toxoplasma gondii requires antigen processing in the endoplasmic reticulum. Nat. Immunol. *9*, 937–944.

Celli, J., de Chastellier, C., Franchini, D.M., Pizarro-Cerda, J., Moreno, E., and Gorvel, J.P. (2003). Brucella evades macrophage killing via VirB-dependent sustained interactions with the endoplasmic reticulum. J. Exp. Med. *198*, 545–556.

Delamarre, L., Pack, M., Chang, H., Mellman, I., and Trombetta, E.S. (2005). Differential lysosomal proteolysis in antigen-presenting cells determines antigen fate. Science *307*, 1630–1634.

Gagnon, E., Duclos, S., Rondeau, C., Chevet, E., Cameron, P.H., Steele-Mortimer, O., Paiement, J., Bergeron, J.J., and Desjardins, M. (2002). Endoplasmic reticulum-mediated phagocytosis is a mechanism of entry into macrophages. Cell *110*, 119–131.

Ghanem, E., Fritzsche, S., Al-Balushi, M., Hashem, J., Ghuneim, L., Thomer, L., Kalbacher, H., van Endert, P., Wiertz, E., Tampé, R., and Springer, S. (2010). The transporter associated with antigen processing (TAP) is active in a post-ER compartment. J. Cell Sci. *123*, 4271–4279.

Goldszmid, R.S., Coppens, I., Lev, A., Caspar, P., Mellman, I., and Sher, A. (2009). Host ER-parasitophorous vacuole interaction provides a route of entry for antigen cross-presentation in Toxoplasma gondii-infected dendritic cells. J. Exp. Med. *206*, 399–410.

Gubbels, M.J., Striepen, B., Shastri, N., Turkoz, M., and Robey, E.A. (2005). Class I major histocompatibility complex presentation of antigens that escape from the parasitophorous vacuole of Toxoplasma gondii. Infect. Immun. *73*, 703–711.

Guermonprez, P., Saveanu, L., Kleijmeer, M., Davoust, J., Van Endert, P., and Amigorena, S. (2003). ER-phagosome fusion defines an MHC class I cross-presentation compartment in dendritic cells. Nature *425*, 397–402.

Hatsuzawa, K., Hirose, H., Tani, K., Yamamoto, A., Scheller, R.H., and Tagaya, M. (2000). Syntaxin 18, a SNAP receptor that functions in the endoplasmic reticulum, intermediate compartment, and cis-Golgi vesicle trafficking. J. Biol. Chem. *275*, 13713–13720.

Hatsuzawa, K., Tamura, T., Hashimoto, H., Hashimoto, H., Yokoya, S., Miura, M., Nagaya, H., and Wada, I. (2006). Involvement of syntaxin 18, an endoplasmic reticulum (ER)-localized SNARE protein, in ER-mediated phagocytosis. Mol. Biol. Cell *17*, 3964–3977.

Hatsuzawa, K., Hashimoto, H., Hashimoto, H., Arai, S., Tamura, T., Higa-Nishiyama, A., and Wada, I. (2009). Sec22b is a negative regulator of phagocytosis in macrophages. Mol. Biol. Cell *20*, 4435–4443.

Hochweller, K., Striegler, J., Hämmerling, G.J., and Garbi, N. (2008). A novel CD11c.DTR transgenic mouse for depletion of dendritic cells reveals their requirement for homeostatic proliferation of natural killer cells. Eur. J. Immunol. *38*, 2776–2783.

Houde, M., Bertholet, S., Gagnon, E., Brunet, S., Goyette, G., Laplante, A., Princiotta, M.F., Thibault, P., Sacks, D., and Desjardins, M. (2003). Phagosomes are competent organelles for antigen cross-presentation. Nature *425*, 402–406.

Howe, C., Garstka, M., Al-Balushi, M., Ghanem, E., Antoniou, A.N., Fritzsche, S., Jankevicius, G., Kontouli, N., Schneeweiss, C., Williams, A., et al. (2009). Calreticulin-dependent recycling in the early secretory pathway mediates optimal peptide loading of MHC class I molecules. EMBO J. *28*, 3730–3744.

Jancic, C., Savina, A., Wasmeier, C., Tolmachova, T., El-Benna, J., Dang, P.M., Pascolo, S., Gougerot-Pocidalo, M.A., Raposo, G., Seabra, M.C., and Amigorena, S. (2007). Rab27a regulates phagosomal pH and NADPH oxidase recruitment to dendritic cell phagosomes. Nat. Cell Biol. *9*, 367–378.

Kagan, J.C., Murata, T., and Roy, C.R. (2005). Analysis of Rab1 recruitment to vacuoles containing Legionella pneumophila. Methods Enzymol. *403*, 71–81.

Kovacsovics-Bankowski, M., and Rock, K.L. (1995). A phagosome-to-cytosol pathway for exogenous antigens presented on MHC class I molecules. Science *267*, 243–246.

Laurent-Matha, V., Derocq, D., Prébois, C., Katunuma, N., and Liaudet-Coopman, E. (2006). Processing of human cathepsin D is independent of its catalytic function and auto-activation: involvement of cathepsins L and B. J. Biochem. *139*, 363–371.

Lin, M.L., Zhan, Y., Proietto, A.I., Prato, S., Wu, L., Heath, W.R., Villadangos, J.A., and Lew, A.M. (2008). Selective suicide of cross-presenting CD8+ dendritic cells by cytochrome c injection shows functional heterogeneity within this subset. Proc. Natl. Acad. Sci. USA *105*, 3029–3034.

Machner, M.P., and Isberg, R.R. (2006). Targeting of host Rab GTPase function by the intravacuolar pathogen Legionella pneumophila. Dev. Cell *11*, 47–56.

McNew, J.A., Parlati, F., Fukuda, R., Johnston, R.J., Paz, K., Paumet, F., Söllner, T.H., and Rothman, J.E. (2000). Compartmental specificity of cellular membrane fusion encoded in SNARE proteins. Nature *407*, 153–159.

Melo, E.J., and de Souza, W. (1997). Relationship between the host cell endoplasmic reticulum and the parasitophorous vacuole containing Toxoplasma gondii. Cell Struct. Funct. *22*, 317–323.

Moffat, J., Grueneberg, D.A., Yang, X., Kim, S.Y., Kloepfer, A.M., Hinkle, G., Piqani, B., Eisenhaure, T.M., Luo, B., Grenier, J.K., et al. (2006). A lentiviral RNAi library for human and mouse genes applied to an arrayed viral high-content screen. Cell *124*, 1283–1298.

Ray, K., Bobard, A., Danckaert, A., Paz-Haftel, I., Clair, C., Ehsani, S., Tang, C., Sansonetti, P., Tran, G.V., and Enninga, J. (2010). Tracking the dynamic interplay between bacterial and host factors during pathogen-induced vacuole rupture in real time. Cell. Microbiol. *12*, 545–556.

Saveanu, L., Carroll, O., Weimershaus, M., Guermonprez, P., Firat, E., Lindo, V., Greer, F., Davoust, J., Kratzer, R., Keller, S.R., et al. (2009). IRAP identifies an endosomal compartment required for MHC class I cross-presentation. Science *325*, 213–217.

Savina, A., and Amigorena, S. (2007). Phagocytosis and antigen presentation in dendritic cells. Immunol. Rev. *219*, 143–156.

Savina, A., Jancic, C., Hugues, S., Guermonprez, P., Vargas, P., Moura, I.C., Lennon-Duménil, A.M., Seabra, M.C., Raposo, G., and Amigorena, S. (2006). NOX2 controls phagosomal pH to regulate antigen processing during crosspresentation by dendritic cells. Cell *126*, 205–218.

Savina, A., Peres, A., Cebrian, I., Carmo, N., Moita, C., Hacohen, N., Moita, L.F., and Amigorena, S. (2009). The small GTPase Rac2 controls phagosomal alkalinization and antigen crosspresentation selectively in CD8(+) dendritic cells. Immunity *30*, 544–555.

Savina, A., Vargas, P., Guermonprez, P., Lennon, A.M., and Amigorena, S. (2010). Measuring pH, ROS production, maturation, and degradation in dendritic cell phagosomes using cytofluorometry-based assays. Methods Mol. Biol. *595*, 383–402.

Sibley, L.D., Niesman, I.R., Parmley, S.F., and Cesbron-Delauw, M.F. (1995). Regulated secretion of multi-lamellar vesicles leads to formation of a tubulo-vesicular network in host-cell vacuoles occupied by Toxoplasma gondii. J. Cell Sci. *108*, 1669–1677.

Slot, J.W., and Geuze, H.J. (2007). Cryosectioning and immunolabeling. Nat. Protoc. *2*, 2480–2491.

Südhof, T.C., and Rothman, J.E. (2009). Membrane fusion: grappling with SNARE and SM proteins. Science *323*, 474–477.

Sugawara, S., Abo, T., and Kumagai, K. (1987). A simple method to eliminate the antigenicity of surface class I MHC molecules from the membrane of viable cells by acid treatment at pH 3. J. Immunol. Methods *100*, 83–90.

Touret, N., Paroutis, P., Terebiznik, M., Harrison, R.E., Trombetta, S., Pypaert, M., Chow, A., Jiang, A., Shaw, J., Yip, C., et al. (2005). Quantitative and dynamic assessment of the contribution of the ER to phagosome formation. Cell *123*, 157–170.

Trombetta, E.S., Ebersold, M., Garrett, W., Pypaert, M., and Mellman, I. (2003). Activation of lysosomal function during dendritic cell maturation. Science *299*, 1400–1403.

Ungermann, C., Sato, K., and Wickner, W. (1998). Defining the functions of trans-SNARE pairs. Nature *396*, 543–548.

Wearsch, P.A., and Cresswell, P. (2007). Selective loading of high-affinity peptides onto major histocompatibility complex class I molecules by the tapasin-ERp57 heterodimer. Nat. Immunol. *8*, 873–881.

Xu, D., Joglekar, A.P., Williams, A.L., and Hay, J.C. (2000). Subunit structure of a mammalian ER/Golgi SNARE complex. J. Biol. Chem. *275*, 39631–39639.

Zhang, T., and Hong, W. (2001). Ykt6 forms a SNARE complex with syntaxin 5, GS28, and Bet1 and participates in a late stage in endoplasmic reticulum-Golgi transport. J. Biol. Chem. *276*, 27480–27487.